

Both reviewers have provided very helpful insights and we concur with all of the reviewers suggestions. A complete point-by-point reply is provided below, along with changes to the manuscript where appropriate. The authors graciously thank the reviewers for the time and effort in enhancing the quality of this work.

Reviewer #1:

General Comments: The manuscript describes a substantial improvement in the return of the Langley ozone lidar system. The manuscript discusses the improvement of the LMOL data retrieval in the lowest 1km by using an OAP (off axis parabolic) reflector. The article describes the technical make-up and design change to the system to incorporate the OAP then justifies the changes by showing robust results from the OWLETS (southeast VA) campaign. The lidar showed higher ozone on average than ozonesondes, but lower than the insitu measurements provided by a UAV holding a POM.

The low level return is an important improvement in the information gathered by the system. The vertical transport and evolution of ozone in the lowest levels of the atmosphere is most pertinent to the evolution of surface concentrations, which most directly impact human health, monitoring, and ultimately policy. While the overall evolution of the boundary layer provides important information to the evolution of surface ozone the ability to properly resolve the near-surface layer is imperative for fine scale dynamics which transpire near the ground. This manuscript provides a technically driven discussion on the set-up of the near-field retrieval, and then displays its practicality in an operational environment, demonstrating the usefulness of the improvement. The manuscript itself seems well written, quite technical for those unfamiliar with the intricacies of the lidar design, but otherwise well structured with good flow with only minor science questions/suggestions and a few technical corrections.

Sciences Questions/Suggestions: Page 2 line 24: "(F#=1)" Does this mean the fnumber of the OAP is 1? The notation caught me a bit off-guard as f-number hadn't been discussed prior to this.

Thank you for the suggested change, for better clarity text changed to "f-number 1.0".

Page 4 line 5: Where does the background value come from?

Added for clarity, the background subtraction is obtained from above 6km for the near-field receiver data, where residual signal effects are insignificant. (Page 4 line 7)

Page 4 line 9: How do you know pressure and temperature at altitude? Do you use a rawinsonde?

Text was added to better explain the pressure and temperature sources:

Ozone cross sections along with pressure and temperature information are used as part of the process to extract ozone mixing ratio as a function of altitude. Pressure and temperature are determined as a function of altitude using a radiosonde; each ozonesonde launch includes a radiosonde. The ozonesonde launches associated with the present data are frequent enough (> 2 per day) to have a better than 3% error due to pressure and temperature uncertainties. In general, LMOL uses the GEOS-5, near real time data product (Putman et. al, 2011) to retrieve pressure and temperature when no radiosonde data can be used. (Page 4, Line 10)

Page 5, lines 8-15: This section shows the capability of the OAP and ozone lidar well.

However, there are a lot of assumptions, so the interpretation should be handled with care. Overall questions and suggestions in this section do not change the conclusion that the new OAP adds incredible value to the lidar, but that additional instrumentation complimenting the lidar can add huge explanatory value to the ozone observed.

We agree with the reviewer that a correct interpretation requires complementary data. We modified the text (see next answer), to provide additional context.

line 8: It is not entirely clear on the figure how the boundary layer collapses. Are you referring to a collapsing of ozone to the surface or collapsing in total depth? If the former, is that collapse hidden behind the UAV observations rectangles near the surface and ozone has mixed down from 400m to the surface around 20UTC? From the surface observations at the bottom of the figure, it looks like ozone has increased by 18UTC thus more likely the collapse refers the PBL total depth decreasing, to the drop in ozone concentrations above 500m, and the enhancement in ozone centered around 400m at the same time. Is that enhancement at 400m due to this collapse or is it possibly due to advection? Did ceilometers capture a PBLH decrease? These

questions are beyond the scope of this paper's purpose, but important to recognize.

As the reviewer noted, these questions are beyond the defined scope of the paper, however, we have added some sentences to provide some additional context on the convective boundary layer collapse.

A collapse in boundary layer can be seen at ~20 UTC (4 pm local time) which contributes to the formation of a more defined enhanced ozone layer (up to 95ppbv) approximately 400 meters above the surface. This remains as a residual layer into the evening, possibly contributing to some marginal ozone enhancement at the surface until 4 UTC. The sonde wind speed data were stagnant at this time, a significant rapid reduction in surface temperature was noted, and the ceilometer reported a corresponding layer height change, with its PBL height product significantly dropping at 20 UTC to 500 meters above the surface, consistent with the ozone layer height change. Further study would be needed to determine if the ozone enhancement at 400 meters is due solely to the mixed layer collapse or other complex changes over short spatial scales, such as effects from the adjacent shipping channel or other nearby sources. (Page 5 line 13)

Figures 4 & Table 1: It was not initially clear that the flights listed in table 1 were the same as those in figure 4. Matching the times and/or titling the profiles in Figure 4 as "Flight #" could help the reader.

Changed titles to date and time in Figure 4. Table 1 changed due to Reviewer #2's suggestions.

Page 7 line 3: Does "all-profile" mean 120m – 1.0 km? Connecting table 1 to figure 4 would help clarify that.

Changed wording and updated table and figure to better represent profiles differences. Please see additional comments under reviewer #2 for additional response.

Page 8 line 9: Flight 4 is also closest to dawn, when heterogeneity is typically greatest. That, plus any low level jet could create large spatial differences reflected in differences between sonde and lidar.

Thank you for the observation—this comment will be included to this paragraph. (Page 9 line 11)

Technical concerns: Page 2 line 28: "Sheer Plate". "Shear Plate" seems to be another possible spelling.

Correct, changed to "shear". (Page 2 line 31)

Page 3: Figures 1 and 2. Are the figure captions switched under the figures? At the very least, it may be prudent to have "Figure 1" first (on the left) and "Figure 2" (on the right of the page).

Figure #s incorrect, switched to make more accurate.

Page 3 line 16: Comma necessary after FOV? Also, I assume FOV means field of view, but this hasn't been defined in the text.

Changed to field of view and no comma.

Page 3 line 21-23: Strangely worded or missing a word...maybe meant to say

"...optimized for the near field. . ." ?

Erased last few words. "alignment was refined" explains that the alignment was optimized.

Page 4 line 11: Unclear if this was meant to be a new paragraph.

Formatting error. Combined correct paragraphs.

Page 5, line 13 – 14: Is that supposed to be Aug 2?

Yes, thank you. We have correct that sentence to say Aug. 2.

Page 8, line 14: "...larger than the than the. . ."

Corrected.

Page 8, line 15: "...but could be potentially be. . ."

Corrected.

Page 8, line 21 - more efficient to eliminate "in another paper" and take "Gronoff et al., 2018" out of parentheses?

Corrected.

Page 8, line 34 - I think there is a word missing: "measurements due use of"

Due to the use of, correct.

Anonymous Referee #2

Received and published: 9 October 2018

Review of “Demonstration of an off-axis parabolic receiver for near-range retrieval of lidar ozone profiles” by Farris et al.

General Comments: The authors report on significant upgrades to the Langley Mobile Ozone Lidar (LMOL) system, particularly the addition of a new receiver to allow the retrieval of near-surface ozone values down to 0.1 km. Comparisons with ozonesonde and POM profile measurements validate the near-field lidar measurements during the OWLETS air quality campaign in summer 2017. The paper has spelling and technical errors, but is otherwise generally well written, and the technical description of the upgraded lidar system and ozone profile validation makes this suitable for AMT. I have minor corrections and one figure suggestion to be addressed, after which I recommend publication.

Discussion paper

Specific Comments: Abstract: Please quote some statistics that describe the lidar comparisons with the ozonesondes and POM measurements. There is currently no description of the results in the abstract.

Thank you, text was added to include more information in the abstract.

Figures 3 and 4: The lidar appears to have a consistent high bias compared to the ozonesondes from ~400-600 m on 2 August. Care to speculate on the causes?

Thank you, we appreciate your comment. We noticed this too but previously avoided speculation. A more rigorous observation study under more stable atmospheric conditions would be needed to really resolve this question. We added an additional plot in Figure 4 showing % difference as a function of height for all flights with propagated uncertainties. For the case with the largest deviation at 500 m, we found using the lidar profile 20 minutes prior to the sonde launch shows a significant improvement in

the 500 m region, supporting the theory that spatial variability in slightly different sampling volume is a significant factor. We added some additional text on this in the error discussion section. (Page 9 line 1)

Table 1: What exactly is being compared here (an average over particular altitudes)?

I don't find a comparison of the average values to be very helpful and I think Table 1 should be replaced by a figure. A more useful comparison would be to take the profiles from Figure 4 and present profiles of the percentage or mixing ratio differences. The 4.43% mean difference quoted on Page 7 is made up of compensating low and high biases in the profile comparisons.

In the original table, we are comparing column averaged data to determine if an overall general bias exists between the profile and sonde. While still useful, we agree with the reviewer that additional information regarding height differences is appropriate. We added an additional plot to figure 4, showing % differences as a function of height for each flight, as well as the average of the flight differences. In the table we have added additional absolute difference information, and included some additional text descriptions to better define and clarify the analysis. These changes have been added primarily in the description for Figure 4, and error analysis sections. In addition, the values previously reported are based on a slightly outdated processing routine from 2017 with some known minor issues with the analog to photon counting merge routine. We had time recently to reprocess the data and used this as an opportunity to reevaluate sonde differences, resulting in an update of all profiles and table data. The results are essentially the same as before, but with a small decrease on 0.1-1 km column reported sonde-lidar bias value (now 2.3% instead of prior 4.3%).

Technical Corrections: Page 1, Line 21: "can cause. . ."

Corrected

Page 1, Line 22: "the elderly. . ."

Corrected

Page 1, Line 23 (and other places, please review): Passive voice, suggest rewriting sentence.

Corrected

Page 1, Line 26: "insights into boundary layer and free troposphere dynamics, providing a. . ."

Corrected

Page 1, Line 29: “measuring ozone from the ground level to stratospheric altitudes.”

Corrected

Page 2, Line 11: Stick with cm, not inches.

Corrected

Page 2, Lines 13-14: Suggested rewrite – “. . . LMOL instrument in a small, compact form, and, unlike traditional refractive elements, is able to simultaneously measure green and UV wavelengths more easily.” Please check.

Corrected

Page 2, Line 23: Need a space between “7.6” and “cm.”

Corrected

Figures 1 and 2: Why is Figure 2 to the left of Figure 1? Did something get switched around? Reverse or renumber the figures, please.

Corrected

Page 3, Lines 5-6: This is not a complete sentence.

“Outputs” in this case is a noun—reworded to help clarify.

Page 3, Line 23: There seems to be a missing word here.

Corrected

Page 3, Line 22: “i.e.” not “ie.”

Page 4, Line 8: Is the temperature and pressure information obtained from the radiosonde data?

Yes, added words to explain. It is also mentioned in the next paragraph.

Page 4, Line 30: “ozonesondes” spelled incorrectly.

Corrected (paragraphs rearranged)

Page 5, Lines 12-13: Assuming you mean Aug. 2 here, not Aug. 1. “in the early morning hours of Aug. 2. . .”

Corrected

Page 5, Lines 14-15: Write as “. . .OAP capability illustrates that the temporal evolution of ozone can be complex, and more clearly reveals how near-surface ozone layers influence surface ozone levels.”

Corrected

Page 7, Line 4: “ozonesonde” spelled incorrectly again here and on Line 15. Please check all instances.

Corrected

Page 7, Line 12: Take out the ampersand and replace with “and.”

Corrected

Page 8, Line 1: Leblanc does not need to be italicized.

Corrected

Page 8, Line 14: Do you mean the biases between the UAV and lidar are of different sign than the ozonesonde/lidar comparisons? Please make this clear.

Line 14 changed “biased opposite” to “biased opposite in sign” to clarify

Page 8, Line 22: “closest in range has the greatest. . .”

Corrected

Page 8, Line 34: “with use of a reflective focusing element” (?) Seems that there is a word missing.

Corrected

Demonstration of an off-axis parabolic receiver for near-range retrieval of lidar ozone profiles

Betsy M. Farris¹, Guillaume P. Gronoff³, William Carrion³, Travis Knepp³, Margaret Pippin², Timothy A. Berkoff²

¹Mechanical Engineering, Colorado State University, Fort Collins, CO 80523, USA
²NASA Langley Research Center, Hampton, VA 23681, USA
³Space Systems & Applications, Hampton, VA 23681, USA

Correspondence to: Timothy A. Berkoff (timothy.a.berkoff@nasa.gov)

Abstract.

During the 2017 Ozone Water Land Environmental Transition Study (OWLETS), the Langley Mobile Ozone Lidar system utilized a new small diameter receiver to improve the retrieval of near-surface signals from 0.1 to 1 km in altitude. This new receiver utilizes a single 90 degree fiber-coupled, off-axis parabolic mirror resulting in a compact form that is easy to align. The single reflective surface offers the opportunity to easily expand its use to multiple wavelengths for additional measurement channels such as visible wavelength aerosol measurements. ~~This unique added capability allows for near field analysis of ozone profile concentrations, enabling the study of near surface pollution dynamics. Results~~Detailed results compare performance of the receiver to both ozonesonde and in-situ measurements from a UAV platform, validating the performance of the near-surface ozone retrievals. ~~The 0.1-1 km lidar column had a 2.3% negative bias and a 7.0% average for the absolute height differences for the ozonesonde flight data obtained, generally falling within known uncertainties. Lidar 0.1-0.2 km measurements had a 10.5% positive bias with respect to UAV data, opposite in direction from the 0.1-1 km column ozonesonde comparisons. A more detailed study under more stable atmospheric conditions would be necessary to resolve the residual instrument differences reported in this work. Nevertheless, this unique added capability is a significant improvement allowing for near-surface observation of ozone.~~

1 Introduction

Tropospheric ozone is a trace gas regulated by the U.S. Environmental Protection Agency due to its harmful impacts to human health and the environment. Specifically, ground level ozone can ~~causes serious problems for sensitive groups such as children, elderly, or those with respiratory diseases (Federal Register Environmental Protection Agency, 2015).~~Formed cause serious problems for sensitive groups such as children, the elderly, or those with respiratory diseases (Federal Register Environmental Protection Agency, 2015). Ozone is ~~formed~~formed as a secondary pollutant from oxides of nitrogen, volatile organic compounds and photochemical reactions often present in metropolitan and densely populated communities. ~~ozone. Ozone~~Ozone must be continuously monitored to comply with current air quality regulations designed to protect the public. Knowing the vertical ozone profile distribution allows for insights into boundary layer ~~dynamics~~dynamics, and free troposphere ~~dynamics~~dynamics, providing a more complete understanding of surface ozone behavior. Therefore it is desirable to have instruments capable of measuring ozone ~~at from~~at from the ground level to stratospheric altitudes.

Formatted: Font color: Auto

Formatted: Font color: Green

The Tropospheric Ozone Lidar Network (TOLNet) was established by NASA to provide needed observations of ozone vertical distribution to better understand pollution dynamics for improving forecast models and satellite retrievals of atmospheric pollutants (Newchurch et al., 2016). The Langley Mobile Ozone Lidar (LMOL), a participating lidar in TOLNet, is a differential absorption lidar system (De Young et al., 2017) that uses a custom pulsed UV laser that generates two wavelengths to obtain vertical profiles of ozone from backscattered light. The system fits into a small mobile trailer and is capable of being operated at remote locations. LMOL has been used in multiple field campaigns (Leblanc et al., 2017; Sullivan et al., 2014; Wang et al., 2017) and provided data for the Ozone Water Land Environmental Transition Study (Sullivan et al., 2018; Berkoff et al., 2017) in summer 2017. The OWLETS campaign aimed to evaluate gradients between water and land in coastal regions, and LMOL provided vertical profiles “over water” by stationing the lidar at the mid-point of the Chesapeake Bay Bridge Tunnel system near the mouth of the Chesapeake Bay. In addition to the UV measurements, this system can also transmit 527 nm light for additional measurements of aerosol and cloud profiles.

One of the key challenges for lidar systems, including those in TOLNet, is recovery of the near-range signals closest to the surface where incomplete transit-receiver geometrical overlap, detector saturation, and other non-linear effects impact the ability to correctly process signals. The Tropospheric Ozone Lidar Network (TOLNet) was established by NASA to provide needed observations of ozone vertical distribution to better understand pollution dynamics for improving forecast models and satellite retrievals of atmospheric pollutants (Newchurch et al., 2016). The Langley Mobile Ozone Lidar (LMOL), a participating lidar in TOLNet, is a differential absorption lidar system (De Young et al., 2017) that uses a custom pulsed UV laser that generates two wavelengths to obtain vertical profiles of ozone from backscattered light. The system fits into a small mobile trailer and is capable of being operated at remote locations. LMOL has been used in multiple field campaigns (Leblanc et al., 2017; Sullivan et al., 2014; Wang et al., 2017) and provided data for the Ozone Water-Land Environmental Transition Study (Sullivan et al., 2018; Berkoff et al., 2017) in summer 2017. The OWLETS campaign aimed to evaluate gradients between water and land in coastal regions, and LMOL provided vertical profiles “over water” by stationing the lidar at the mid-point of the Chesapeake Bay Bridge Tunnel system near the mouth of the Chesapeake Bay. In addition to the UV measurements, this system can also transmit 527 nm light for additional measurements of aerosol and cloud profiles.

One of the key challenges for lidar systems, including those in TOLNet, is recovery of the near-range signals closest to the surface where incomplete transit-receiver geometrical overlap, detector saturation, and other non-linear effects impact the ability to correctly process signals. Secondary smaller diameter receivers with a wider field-of-view are often employed co-aligned with the lidar transmit beam to better recover near-range signals, typically using a single focusing lens (Megie, 1985). In this paper, we describe the use of a unique small-diameter (3”) (Megie, 1985). In this paper, we describe the use of a unique small-diameter (7.62 cm) off-axis parabolic (OAP) fiber-coupled mirror configuration to more easily recover LMOL near-range signals. The OAP approach enables closer range capability

for the LMOL instrument in a small, compact form and, unlike traditional refractive elements, ~~and~~ is able to simultaneously measure green and UV wavelengths more easily.

2 Design and Description of Setup

In previous campaigns prior to 2017, LMOL used a 30 cm diameter Fresnel lens as its near-field receiver. This arrangement had alignment stability issues, was mechanically cumbersome, and could only monitor UV signals. For far field measurements (>800 m range in altitude) a 40 cm diameter Newtonian telescope was used to collect backscattered light and provided stable results in prior campaigns for both UV and green wavelengths. The configuration for the OWLETS 2017 campaign maintained the same far-field telescope, laser transmitter and optics while using a new near-field receiver consisting of a 7.6 cm diameter, 90 degree OAP with a ~~7.6 cm~~ 6 cm focal length (Figure 1). A 1 mm core diameter multimode fiber with a 0.5 numerical aperture matching the fast (~~f#~~ = f-number 1.0) OAP was mounted in an x-y-z positioning stage and aligned to the focus point of the mirror (Figure 2). The fiber core diameter and mirror focal length combination provides a 13.2 mrad full-angle field-of-view, approximately 10 times larger than the existing far-field receiver. Initial fiber alignment of the OAP was done in a laboratory setting using a visible collimated beam verified by an interferometric ~~sheershear~~ plate to position the fiber launch at the focal point of the OAP. The fiber x-y-z position was also verified using an autocollimator to examine the quality of beam collimation from the mirror when the fiber was back-illuminated. Once positioned, the fiber distance and position did not require any course adjustments in the field. The entire assembly was mounted on a two-axis goniometer with the mirror placed looking upward next to the LMOL far-field receiver. The goniometer arrangement allowed for repeatable angular adjustment of the assembly pointing direction for atmospheric alignment to the LMOL transmitted beam. The LMOL transmitted beam is generated by a tunable Ce:LiCAF laser at a 1 kHz pulse repetition rate, with 0.1 mJ/pulse. Pulse-to-pulse wavelength switching is accomplished with rapid tuning the Ce:LiCAF oscillator between 286 and 292 nm across an ozone absorption feature, enabling differential absorption backscatter

measurements of ozone as a function of altitude and time to be obtained (De Young et al., 2017).

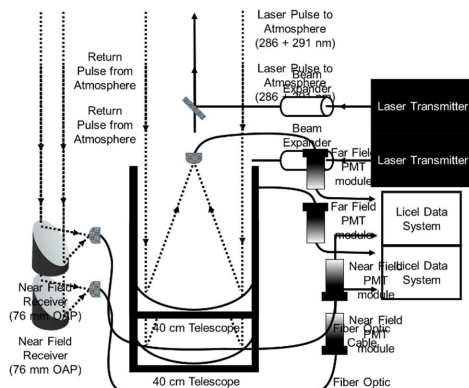


Figure 2: System setup with OAP mirror receiver adjacent to the larger far-field receiver.

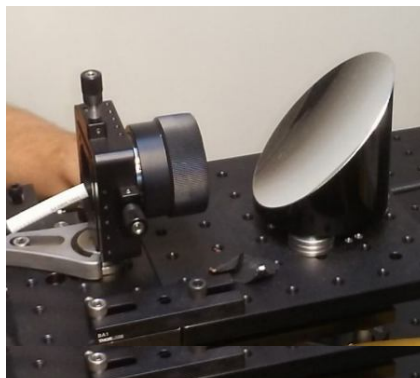


Figure 1: Fiber-coupled OAP configuration.

3 Atmospheric Alignment & Measurements

The fiber outputs of the fibers from the near-field and far-field telescopes were coupled to collimating optics, and UV bandpass filters (280-295 nm spectral window) that which were integrated with Hamamatsu photo-multiplier tube (PMT) detectors in light-tight enclosures. For normal atmospheric science data collection, the outputs of the PMTs were connected to a Licel data system that provided simultaneous analog and photon counting measurements of both the near-field and far-field PMT signals. The Licel system was synchronously gated with the alternating wavelength pulses, so that 286 and 292 nm wavelength profiles are separately captured by the data system memory and subsequently recorded to the computer data acquisition system for processing of raw signals into calibrated ozone profiles.

A two-step process is used to align backscattered signals to the near-range and far-range receivers. First, the far-field receiver signal is optimized by changing the angular adjustments on the last outgoing mirror by monitoring the signal on either an oscilloscope or real-time raw signal display generated by the data acquisition system and fixing the mirror in place. The transmitted beam is placed at the center of the far-field receiver field of view (FOV) by monitoring the real-time signal amplitude at a range-bin in the upper free troposphere (typically 3-5 km altitude) and centering the mirror adjustments on the maximum signal level. After alignment of the transmitted beam to the far-field receiver, the second step orients the near-field receiver to the transmit beam using the near-field goniometer mount adjustments. The near-field orientation is then optimized by centering its FOV to the transmit beam by finding the center maximum of the signal in the lower free troposphere (typically 1-1.5 km). Because of the higher noise level of the near-field channel, this alignment was refined with a real-time range integrated (i.e. 1-1.5 km) signal where which required

Formatted: Font color: Auto

Formatted: Font color: Auto

sufficient signal ~~could~~^{could} be obtained over a 2-3 second average ~~optimized the near field receiver alignment.~~ Once both receivers' signals were verified aligned with the laser beam, then atmospheric data would be collected, typically at 20 second temporally averaged profiles at 7.5 meter vertical sampling resolution.

5 The processing of raw profile signals to obtain calibrated ozone profiles is based on the standard DIAL technique described previously (Browell et al., 1985). Raw signals, both analog and photon counting, are background subtracted and range-squared before applying a single-pass Savitzky-Golay filter. Analog and photon-count channels are merged together to provide a single optimized profile for range and signal-to-noise performance. Ozone cross sections along with pressure and temperature information are used as part of the filter process to extract ozone mixing ratio as a function of altitude. The process is repeated for each new profile on a 5 minute temporal averaged basis, to provide a continuous curtain display on the evolution of ozone vertical distribution during the course of a day.

10 LMOL far-field ozone profiles prior to 2017 have been compared with ozonesonde launches and other ozone lidar systems in various field campaigns and cross-validation studies (Leblanc et al., 2018; Sullivan et al., 2014). From these investigations, typical cross-comparisons of the far-field channel fall within +/- 5% of the signal level reported, consistent with propagated errors in the LMOL ozone data products.

15

The summer 2017 OWLETS campaign provided a unique opportunity to demonstrate the capabilities of the new near-range OAP receiver for LMOL. The LMOL lidar system was stationed at the third island of the Chesapeake Bay Bridge Tunnel site (CBBT), to obtain "over water" measurements of ozone. In addition to the lidar, ozonesonde flights were regularly launched from CBBT during the OWLETS campaign. Each ozonesonde flight contained an in-situ instrumentation package consisting of an iMet radiosonde measuring temperature, water vapor, winds, and pressure along with an electrochemical ozone sensor package manufactured by EN-SCI.

20

The processing of raw profile signals to obtain calibrated ozone profiles is based on the standard DIAL technique described previously (Browell et al., 1985). Raw signals, both analog and photon counting, are background subtracted and range-squared before applying a single-pass Savitzky-Golay filter. The background subtraction is obtained from above 6 km for the near-field receiver data, where residual signal effects are insignificant. Analog and photon-count channels are merged together to provide a single optimized profile for range and signal-to-noise performance. Ozone cross sections, along with pressure and temperature information from co-located radiosonde launches, are used as part of the process to extract ozone mixing ratio as a function of altitude. The ozonesonde launches associated with the present data are frequent enough (> 2 per day) to have a better than 3% error due to pressure and temperature uncertainties. In general, LMOL uses the GEOS-5, near real time data product (Putman et. al, 2011) to retrieve pressure and temperature when no ozonesonde/radiosonde data can be used. The process is repeated for each new profile on a 5 minute temporal averaged basis, to provide a continuous curtain display on the evolution of ozone vertical distribution during the course of a day.

25

30

35 LMOL far-field ozone profiles prior to 2017 have been compared with ozonesonde launches and other ozone lidar systems in various field campaigns and cross-validation studies (Leblanc et al., 2018; Sullivan et al., 2014). From

these investigations, typical cross-comparisons of the far-field channel fall within +/- 5-7% of the signal level reported, consistent with propagated errors in the LMOL ozone data products. The summer 2017 OWLETS campaign provided a unique opportunity to demonstrate the capabilities of the new near-range OAP receiver for LMOL. The LMOL lidar system was stationed at the third island of the Chesapeake Bay Bridge Tunnel site (CBBT), to obtain "over-water" measurements of ozone. In addition to the lidar, ozonesonde flights were regularly launched from CBBT during the OWLETS campaign. Each ozonesonde flight contained an in-situ instrumentation package consisting of an iMet radiosonde measuring temperature, water vapor, winds, and pressure along with an electrochemical ozone sensor package manufactured by EN-SCI.

The OAP receiver alignment procedure was optimized during the OWLETS campaign and used to retrieve ozone profiles between 120 and 1000 meters in altitude, nearly the entire atmospheric boundary layer. Values below 120 meters in altitude were significantly influenced by typical near-range non-linear effects and are screened from analysis in a similar fashion that far-field data is screened from 0-400 meters in altitude. Future development of a similar OAP system for even closer-range capability is being considered.

For the OAP performance analysis, OWLETS data taken on Aug 1-2, 2017 represents the most comprehensive inter-comparison opportunity taken during the campaign, with 5 ozonesondes launched during a continuous 32 hour duration of LMOL measurements with the new OAP near-range receiver. In addition, a small drone (UAV) with an in-situ ozone monitor on-board was also flown at this time at the same CBBT location, providing near-range vertical ozone profiles from 0-200 meters in altitude, allowing for additional lidar inter-comparisons on both days. The UAV in-situ ozone sensor consisted of a 2B Technologies model POM device that is an approved Federal Equivalent Method (FEM) and NIST traceable ozone measurement with +/- 2 ppbv or better absolute accuracy, and contained its own built-in data storage, battery, sampling air flow pump, and GPS tracker (2B Technologies, 2016). The POM was mounted to the top structure of the UAV and then flown in different flight patterns to investigate near-range variability in ozone at the CBBT site.

Figure 3 displays the 32 hour data taken by the near-range OAP receiver, overlaid with the ozonesonde, UAV and surface in-situ ozone measurements taken in the Aug 1-2 time frame. The vertical resolution of the lidar data changes with altitude by an adaptive smoothing technique that is described in work detailing a titration event captured during the OWLETS campaign (Gronoff et al., 2018). Data collection started approximately 8 am local time on Aug 1, with surface and near-surface ozone increasing in magnitude as the day progresses. A collapse in boundary layer can be seen at ~20 UTC (4 pm local time) which contributes to the formation of a more defined enhanced ozone layer (up to 95 ppbv) approximately 400 meters above the surface. This remains as a residual layer into the evening, possibly contributing to some marginal ozone enhancement at the surface until 4 UTC. Values at the surface and lowest altitudes then decrease significantly in the early morning Aug 1 hours. The sonde wind speed data were stagnant during this time, a significant rapid reduction in surface temperature was noted, and the ceilometer reported a corresponding layer height change, with its planetary

boundary layer height product significantly dropping at 20 UTC to 500 meters above the surface, consistent with the ozone layer height change. Further study would be needed to determine if the ozone enhancement at 400 meters is due solely to the mixed layer collapse or other complex changes over short spatial scales, such as effects from the adjacent shipping channel or other nearby sources. Values at the surface and lowest altitudes then decrease significantly in the early morning hours of Aug 2 as the elevated layer also somewhat dissipates and also mixes to higher altitudes with the growth of the Aug. 4² boundary layer. This result from the new near-range OAP capability illustrates that the temporal evolution of ozone can be complex, and more clearly ~~reveal~~reveals how near surface ozone layers ~~potential interact with~~influence surface ozone levels.

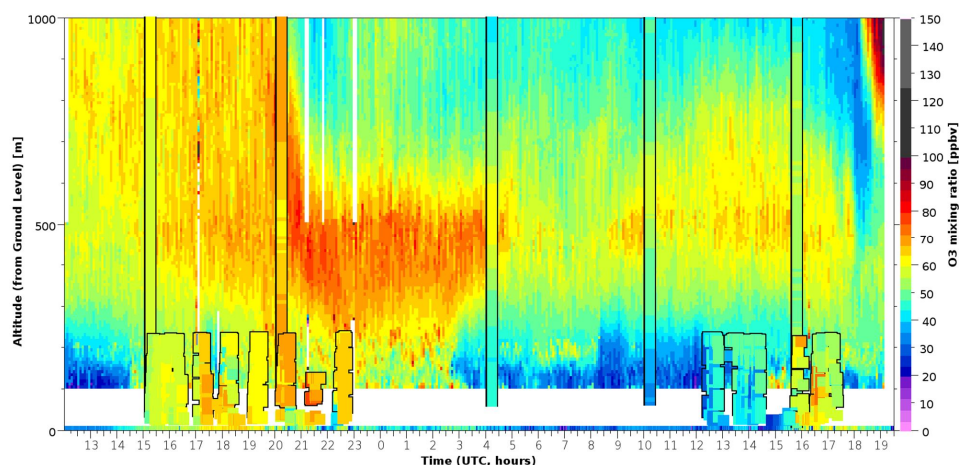
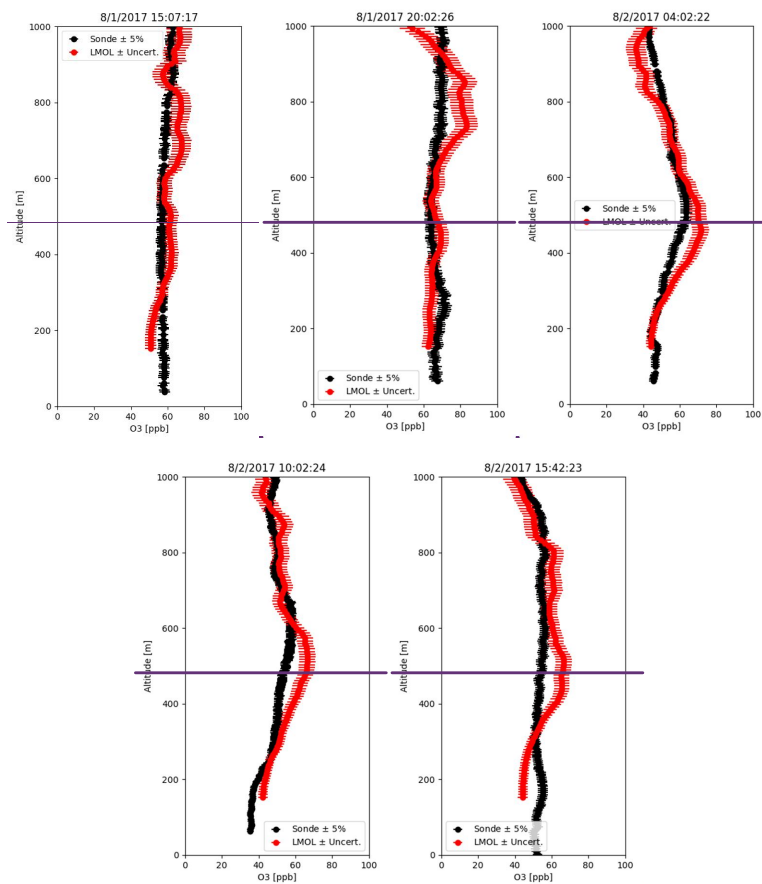


Figure 3: LMOL ozone 32-hour lidar curtain obtained Aug 1-2, overlaid with five ozonesonde measurements and UAV in-situ measurements (0-200 m).

In general, the ozone measurements between lidar, ozonesonde, surface, and UAV were found to be fairly consistent with each other where spatio-temporal coincidences occur. Although differences can occur in ozonesonde-lidar comparisons due to atmospheric sampling discrepancies due to wind advection of the ozonesonde position, as well as the time constant of the electro-chemical sensor. From discussions with the manufacturer, and known ascent rate of the ozonesonde, vertical resolution of the ozonesonde is estimated to be 200 meters.

Figure 4 shows the ozonesonde profiles and corresponding OAP near-range receiver profiles and the corresponding uncertainties. For this comparison, the OAP receiver data was smoothed to 200 meter resolution to match the expected ozonesonde vertical resolution.



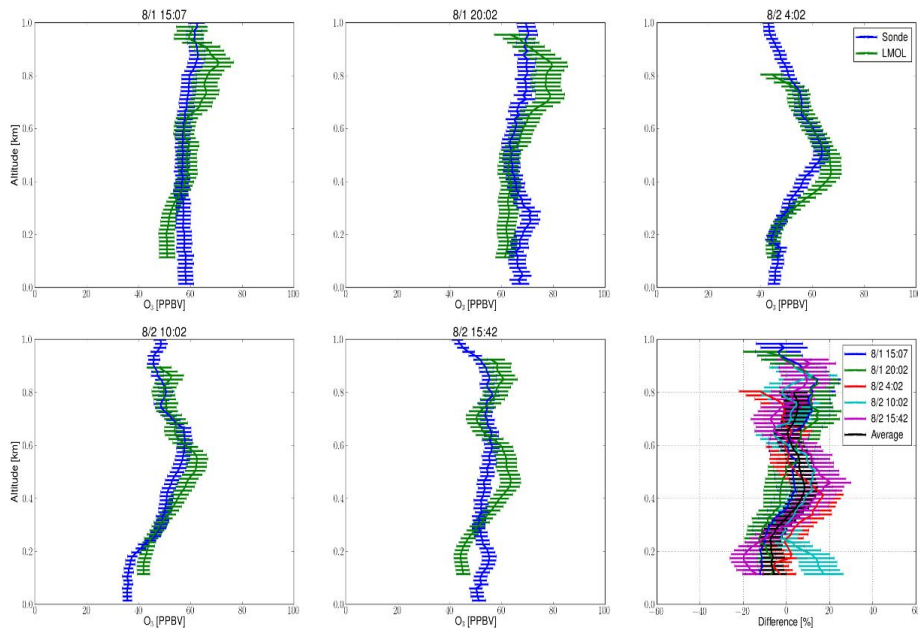


Figure 4: Ozonesonde and LMOL comparison for near field (0-1000 m) and the % height differences for all flights displayed on the bottom right plot.

	Sonde Mean +/- St. Dev.	LMOL Mean +/- St. Dev.	% Difference	Abs. % Difference
Flight 8/1 15:00 UTC	58.54 ± 1.97	60.859.0 ± 4.92	-3.861.0	6.6
Flight 28/1 20:00 UTC	67.32 ± 2.35	69.567.8 ± 6.85	-3.220.9	7.5
Flight 38/2 04:00 UTC	52.754.3 ± 6.26	54.055.9 ± 10.8	-2.448	5.0
Flight 48/2 10:00 UTC	49.06 ± 6.13	53.452.0 ± 7.28	-8.594.9	6.2
Flight 58/2 15:45 UTC	53.154.0 ± 2.63	55.30 ± 7.72	-4.061.8	9.7
		Mean of % Differences	-2.3	7.0

Table 1: Comparison of sonde and LMOL column (0 to 1 km) average ozone values (ppbv), the percent differences (bias), and the percent difference in values absolute differences for Figure 4 flights. The data sample standard deviations are also shown along with the mean values.

Inserted Cells

Formatted: Centered, Line spacing: single, Border: Top: (No border), Bottom: (No border), Left: (No border), Right: (No border), Between : (No border)

Formatted: English (United States)

Formatted: English (United States)

Formatted: English (United States)

Formatted: Line spacing: single, Border: Top: (No border), Bottom: (No border), Left: (No border), Right: (No border), Between : (No border)

Formatted: English (United States)

Formatted: English (United States)

Formatted: English (United States)

Formatted: English (United States)

Formatted: Line spacing: single, Border: Top: (No border), Bottom: (No border), Left: (No border), Right: (No border), Between : (No border)

Formatted: English (United States)

Formatted: English (United States)

Formatted: English (United States)

Formatted: English (United States)

Formatted: Line spacing: single, Border: Top: (No border), Bottom: (No border), Left: (No border), Right: (No border), Between : (No border)

Formatted: English (United States)

Formatted: English (United States)

Formatted: English (United States)

Formatted: English (United States)

Formatted: Line spacing: single, Border: Top: (No border), Bottom: (No border), Left: (No border), Right: (No border), Between : (No border)

Formatted: English (United States)

Formatted: English (United States)

Formatted: English (United States)

Formatted: English (United States)

Formatted

... [1]

Formatted: English (United States)

Formatted: English (United States)

Formatted: English (United States)

Formatted: English (United States)

As can be seen from Table 1, the 0-1 km column bias differences between lidar and sonde are relatively small, with means of the all profile differences being 4.43 on average -2.3%, with the lidar having an overall high bias relative to the sonde launches. While the columnar bias is of interest to assess overall polarity of offset, an absolute columnar bias is also reported in Table 1, determined by taking the absolute difference at each height prior to the mean, to assess magnitude of error irrespective of polarity. This absolute error parameter eliminates difference minimization effects when a positive bias in one part of the profile serves to reduce a negative bias at another location in the profile, providing additional information of differences in column magnitudes.

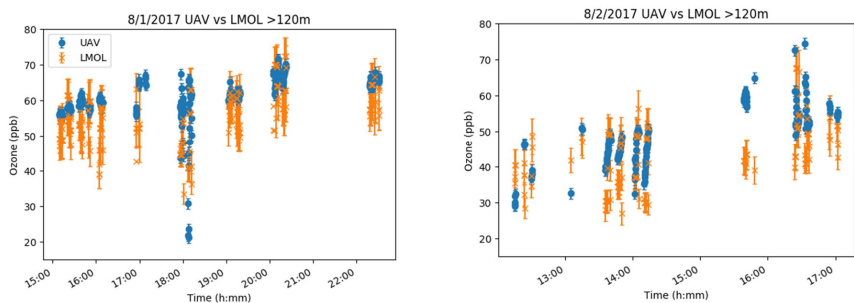


Figure 5: Time Series for 8/1-8/2/2017 of UAV measurements above 120m and the corresponding LMOL data

	UAV Mean +/- St. Dev.	LMOL Mean +/- St. Dev.	% Difference
8/1/2018	60.9 ± 5.92	55.4 ± 7.24	9.46
8/2/2018	48.7 ± 7.76	43.3 ± 8.88	11.63

Table 2: UAV and LMOL comparison for 8/1 and 8/2 for samplings taken above LMOL above 120 m. The data sample standard deviations are also shown along with the mean values.

Although the UAV measurements were limited to 200 m altitude due to FAA airspace regulations, a number of vertical profiles were obtained on Aug 1 and 2, and provide additional inter-comparison with the new OAP near-range receiver in the lowest portion of its altitude range. Figure 5 shows a time series comparison during the Aug 1-2 flights over the lidar and within the altitude range of the receiver. Unlike the ozonesonde, the UAV can be held to a controlled fixed position over the lidar, reducing some of the air-mass sampling issues with the ozonesonde. The ozone concentrations measured by the POM on the UAV averaged 9.46 and 11.63% higher than LMOL measurements for 8/1 and 8/2, respectively.

Error discussion

TOLNet lidar systems have collectively developed rigorous processing algorithms based on Network for the Detection of Atmospheric Composition Change (NDACC) ozone lidar protocols to ensure consistency in O₃ data products and associated uncertainties between instruments [Leblanc et al., 2016a,b, 2016, Leblanc et al., 2018]. The OAP error bars presented in Figure 4 are the errors propagated from these standardized TOLNet/NDACC protocols, and take into

Formatted: Font: Not Bold, English (United States)

Formatted: Font: Not Italic

Formatted: Font: Times New Roman

account random detector noise as well as other uncertainties including O₃ absorption and Rayleigh cross-sections used in determining concentration values. Comparisons with co-located electro-chemical ~~ozonesonde~~ozonesonde flights is a traditional approach used to cross-validate with O₃ lidar profiles, typically limited to 5% absolute accuracy. LMOL's 5 minute profiles have an uncertainty of 7-8% in the 100m-1km range, somewhat larger than the absolute value for the ozonesonde. In Figure 4, the LMOL profiles have been optimized to have a 200m vertical resolution, which corresponds to the ozonesonde resolution. The % difference profiles of all flights in Figure 4 have deviations that appear fairly random in nature, and fall within the propagated errors. The highest bias appears on the last ozonesonde at around 500m; a more detailed study of that event indicates the atmosphere was highly variable at this time frame. A comparison of the lidar profile taken 20 minutes earlier to the same ozonesonde significantly reduces the deviation, suggesting atmospheric spatiotemporal variability as the cause. While the sample standard deviations reported in Table 1 are significant compared to the sonde-lidar difference biases, the per flight 0-1 km mean values allow for higher precision ~~<1 ppbv (<2%)~~ determinations due to the significant number of samples available in the column. This precision improvement allows for better overall assessment of static bias error between the OAP and corresponding sonde data. All sondeSonde-lidar column bias differencesdifference values, except flight #4 (8/2 10:02 UTC), in Table 1 are close to, or fall within the 5% sonde absolute reported accuracy limits. The column averaged propagation of errors following standardized TOLNet protocols for these columns varied between 7.7 to 8. It is also noted that flight #4 percent, somewhat is closest to dawn when atmospheric heterogeneity is typically greatest and may explain some of its larger than the absolute limits of the sonde. Consequently, these residual deviations. In general, the sonde-lidar differences are less than overlap within their expected errors (with the exception of flight #4), indicating agreement to the extent possible within performance limits of the sondeozonesonde and OAP data.

~~However, the~~The UAV-lidar differences in Table 2 are biased opposite in sign and somewhat larger than the than the expected instrument error. The exact cause of the larger UAV-lidar bias remains unclear but could be potentially be attributed to multiple factors. The UAV in-situ sensor provides high temporal resolution (10 seconds) with a very small volume sample compared to the OAP observed air mass. The high degree of short-term signal variability evidenced by the UAV/OAP-Figure 5 time series suggests rapidly changing significant small scale gradients, making the UAV and lidar co-comparison more challenging than anticipated. The near-surface variability is attributed, in part, to large shipping lane traffic adjacent to the CBBT site as well as other factors, as documented in another paper (Gronoff et al., 2018), where large changes in Pandora columnar NO₂ correlated with lidar near-surface ozone titration events. Furthermore, the signal closest in range havehas the greatest potential for instrumental error, and limited height range of the UAV may have revealed an increased error for the lowest few recoverable range bins <200 meters, and suggests the need for further investigation. A more detailed study under more stable atmospheric conditions would be needed to more effectively resolve the residual instrumental biases reported here.

4 Summary

It was determined that the improved receiver setup for LMOL allowed for preliminary validation of ozone lidar measurements at a minimum of 120 m compared to the 800 m minimum of the larger far-field receiver. This

improvement significantly enhances the capability of the LMOL system allowing for a better understanding of low altitude (120-1000 m) ozone atmospheric dynamics that are critical in evaluating atmospheric models and air pollution satellite retrievals. The new fiber-coupled OAP receiver offers the benefit of small compact form; and can be adapted more easily to aerosol visible wavelength measurements due to the use of a reflective focusing element. Such a measurement can be possible by using a dichroic ~~beam splitter~~beamsplitter at the fiber output to separate green ~~backscattered~~backscattered light from the laser pump of the current system to measure the light separately from the UV retrieval. Comparison measurements with ozonesonde and UAV measurements show good agreement with the ozone values obtained from the new receiver. LMOL values were biased above the ozonesonde measurements but biased below the UAV measurements, ~~demonstrating reasonable agreement but generally fall within known~~uncertainties. This new measurement capability for LMOL improvements will continue to further the goals of TOLNet, allowing for development of more compact lower-cost lidar systems with near-range measurement capabilities.

Data Availability All data for the OWLETS campaign is publically available at the campaign's website, <https://www-air.larc.nasa.gov/missions/owlets/index.html>

Acknowledgements:

This work was supported in part by the NASA Science Innovation Fund, NASA Tropospheric Composition Program, and the TEMPO Student Collaboration project with funding provided through the NASA Science Mission Directorate Earth System Science Pathfinder program. Special thanks to an exceptional group of student interns that provided support that made ~~ozonesonde~~ozonesonde and UAV measurements possible during OWLETS: Lance Nino, Lindsey Rodio, Jeremy Schroeder, Pablo Sanchez, Emily Gargulinski, Marlia Harnden, Desorae Davis, and Angela Atwater. Thanks to Danette Allen, Eddie Adcock, Zak Johns, Mark Motter, Jim Neilan, and Matt Vaughan of the NASA LaRC UAV team. This work could also not have been completed without the helpful accommodations of Edward Spencer and the management and employees with the Chesapeake Bay Bridge and Tunnel District. A final thanks goes to Tim Berkoff, Guillaume Gronoff, Margaret Pippin and the other OWLETS PIs for their excellent mentorship and support.

References:

- 2B Technologies: POM, personal ozone monitor., 1(303), 5–7 [online] Available from: <http://www.twobtech.com/pom-personal-ozone-monitor.html>, 2016.
- Berkoff, T., Sullivan, J., Pippin, M. R., Gronoff, G., Knepp, T. N., Twigg, L. W., Schroeder, J., Carrion, W., Farris, B., Kowalewski, M. G., Nino, L., Gargulinski, E., Langley, U., Rodio, L., Sanchez, P., Davis, A. A. D., Janz, S. J., Judd, L., Pusede, S., Wolfe, G. M., Stauffer, R. M., Munyan, J., Flynn, J., Moore, B., Dreessen, J., Salkovitz, D., Stumpf, K., King, B., Hanisco, T. F., Brandt, J., Blake, D. R., Abuhassan, N., Cede, A., Tzortziou, M., Demoz, B., Tsay, S.-C., Swap, R., Holben, B. N., Szykman, J., McGee, T. J., Neilan, J. and Allen, D.: Overview

- of the Ozone Water-Land Environmental Transition Study: Summary of Observations and Initial Results, in American Geophysical Union, Fall Meeting 2017, American Geophysical Union, Fall Meeting 2017, New Orleans, LA. [online] Available from: <https://agu.confex.com/agu/fm17/meetingapp.cgi/Paper/246428>, 2017.
- 5 Browell, E. V., Ismail, S. and Shipley, S. T.: Ultraviolet DIAL measurements of O₃ profiles in regions of spatially inhomogeneous aerosols., *Appl. Opt.*, 24(17), 2827–36, doi:10.1364/AO.24.002827, 1985.
- Federal Register Environmental Protection Agency: National Ambient Air Quality Standards for Ozone Final Rule, 40 CFR Parts 50,51,52,53 58, 80(206), 1–7 [online] Available from: <https://www.federalregister.gov/documents/2015/10/26/2015-26594/national-ambient-air-quality-standards-for-ozone>, 2015.
- 10 Gronoff, G., et al : A Method for Observing Near Range Point Source Induced O₃ Titration Events Using Co-located Lidar and PANDORA measurements, Submitted to Atmospheric Environment, 2018.
- Leblanc, T., Brewer, M. A., Wang, P. S., Granados-Muñoz, M. J., Strawbridge, K. B., Travis, M., Firanski, B., Sullivan, J. T., McGee, T. J., Sumnicht, G. K., Twigg, L. W., Berkoff, T. A., Carrion, W., Gronoff, G., Aknan, A., Chen, G., Alvarez, R. J., Langford, A. O., Senff, C. J., Kirgis, G., Johnson, M. S., Kuang, S., and Newchurch, M. J.: Validation of the TOLNet ~~Lidars~~ Lidars: the Southern California Ozone Observation Project (SCOOP), *Atmos. Meas. Tech. Discuss.*, 11, 6137–6162, <https://doi.org/10.5194/amt-11-6137-2018-240>, in review, 2018.
- 15 Leblanc, T., Sica, R. J., van Gijzel, J. A. E., Godin-Beekmann, S., Haefele, A., Trickl, T., Payen, G. and Liberti, G.: Proposed standardized definitions for vertical resolution and uncertainty in the NDACC lidar ozone and temperature algorithms – Part 2: Ozone DIAL uncertainty budget, *Atmos. Meas. Tech.*, 9(8), 4051–4078, doi:10.5194/amt-9-4051-2016, 2016.
- 20 Leblanc, T., Senff, C. J., Sullivan, J., Berkoff, T., Gronoff, G., Strawbridge, K. B., Portafaix, T., Duflot, V. and McGee, T. J.: Using a Centralized Lidar Data Processing Algorithm As a Reference Transfer for the Intercomparison of Campaign Data: Examples from the TOLNet SCOOP and the NDACC MORGANE Campaigns, in American Meteorological Society, 97th Annual Meeting, Seattle, WA. [online] Available from: https://ams.confex.com/ams/97Annual/video gateway.cgi/id/36928?recordingid=36928&uniqueid=Paper310453&entry_password=327228, 2017.
- 25 Megie, G.: Laser Remote Sensing: Fundamentals and Applications, *Eos, Trans. Am. Geophys. Union*, 66(40), 686, doi:10.1029/EO066i040p00686-05, 1985.
- 30 Newchurch, M., Saadi, J. A. Al, Alvarez, R. J., Burris, J., Cantrell, W., Chen, G., Deyoung, R., Hardesty, R. M., Hoff, R. M., Kaye, J. A., Kuang, S., Langford, A., Leblanc, T., Mcdermid, S., McGee, T. J., Pierce, R. B., Senff, C. J., Sullivan, J., Szykman, J., Tonnesen, G. and Wang, L.: Tropospheric Ozone Lidar Network (TOLNet) - Long-term Tropospheric Ozone and Aerosol Profiling for Satellite Continuity and Process Studies, *EPJ Web Conf.*, 119, 20001, 4, doi:<https://doi.org/10.1051/epjconf/201611920001>, 2016.
- 35 Putman, W. M. and Suarez, M.: Cloud-system resolving simulations with the NASA Goddard Earth Observing System global atmospheric model (GEOS-5), *Geophys. Res. Lett.*, 38(16), 1–5, doi:10.1029/2011GL048438, 2011.

Sullivan, J.T, et al. The Ozone Water-Land Environmental Transition Study (OWLETS):
An Innovative Strategy for Understanding Chesapeake Bay Pollution Events, Bulletin of the American
Meteorological Society, submitted.

Sullivan, J. T., McGee, T. J., Sumnicht, G. K., Twigg, L. W. and Hoff, R. M.: A mobile differential absorption lidar
to measure sub-hourly fluctuation of tropospheric ozone profiles in the Baltimore-Washington, D.C. region,
Atmos. Meas. Tech., 7(10), 3529–3548, doi:10.5194/amt-7-3529-2014, 2014.

Wang, L., Newchurch, M. J., Alvarez, R. J., Berkoff, T. A., Brown, S. S., Carrion, W., De Young, R. J., Johnson, B.
J., Ganoe, R., Gronoff, G., Kirgis, G., Kuang, S., Langford, A. O., Leblanc, T., McDuffie, E. E., McGee, T. J.,
Pliutau, D., Senff, C. J., Sullivan, J. T., Sumnicht, G., Twigg, L. W. and Weinheimer, A. J.: Quantifying
TOLNet ozone lidar accuracy during the 2014 DISCOVER-AQ and FRAPPÉ campaigns, Atmos. Meas. Tech.,
10(10), 3865–3876, doi:10.5194/amt-10-3865-2017, 2017.

De Young, R., Carrion, W., Ganoe, R., Pliutau, D., Gronoff, G., Berkoff, T. and Kuang, S.: Langley mobile ozone
lidar: ozone and aerosol atmospheric profiling for air quality research, Appl. Opt., 56(3), 721–730,
doi:10.1364/AO.56.000721, 2017.

Zhang, Y., Yi, F., Kong, W. and Yi, Y.: Slope characterization in combining analog and photon count data from
atmospheric lidar measurements, Appl. Opt., 53(31), 7312, doi:10.1364/AO.53.007312, 2014.

Formatted: Indent: Left: 0", Hanging: 0.25"

Line spacing: single, Border: Top: (No border), Bottom: (No border), Left: (No border), Right: (No border), Between : (No border)